

Department of Precision and Microsystems Engineering

Ringdown of high-Q nonlinear Si_3N_4 beam resonator with multi-overtone recording

Bart Schoone

Report no : 2024.010
Coach : Dr. A. Keşkekler
Professor : Dr. F. Alijani, Dr. R.A. Norte
Specialisation : Dynamics of Micro- and Nanosystems (DMN)
Type of report : MSc.Thesis
Date : Februari 10, 2024

Ringdown of high-Q nonlinear Si_3N_4 beam resonator with multi-overtone recording

by

Bart Schoone

Student Number: 4473329
Professor: Dr. F. Alijani, Dr. R.A. Norte
Daily supervisor: Dr. A. Keşkekler
Date: Saturday 10th February, 2024
Specialisation: Dynamics of Micro- and Nanosystems (DMN) Faculty:
3mE, Delft Report no: 2024.010

Preface

Dear reader,

My fascination with mechanical systems led me to study Mechanical Engineering. While the Bachelor's degree largely focuses on solving linear and often undamped systems, the Master's is less permissible. My introduction to the domain of nonlinear dynamics came through the lectures held by Farbod during the Engineering Dynamics course, and later in Nonlinear Dynamics. His enthusiasm and clear presentation style inspired me to pursue my graduation project in this field.

When asked for possibilities, Farbod offered endless research topics and introduced me to the remarkable properties of graphene combined with tunable nonlinear damping. The last one caught my attention. Like many students, I encountered challenges throughout this project. The vastness of the subject, shifts from graphene to silicon nitride, days in the lab with fruitless results, or the multifaceted interpretation of measurements all posed as impediments. I am grateful for the invaluable discussions and advice from Ata and Farbod. Your guidance and encouragement helped me navigate through setbacks and witness the progress, no matter how incremental it seemed.

This project would not be possible without the support of my friends, siblings and, of course, my parents, who patiently awaited for this moment. Their unwavering support sustained through the journey. Thank you all. In closing, dear reader, while this research may appear inconclusive, and far from flawless, I hope it contributes a little to the understanding of the intricate dynamics of micro- and nanosystems. Thank you all.

Bart Schoone
Delft, February 2024

Summary

Micro- and nanoelectromechanical (MEM/NEM) resonators are used in numerous fields of engineering and are crucial for time keeping, synchronization, and sensing applications. These systems are inherently subjected to energy dissipation, which is a limiting factor in the performance. Extensive understanding is essential when nonlinearities show up in both stiffness and dissipation, to design appropriately. Focusing on dissipative mechanisms, this thesis explores the vibrational behavior of a suspended clamped-clamped beam fabricated from silicon-nitride. This study reveals a notorious decay in ringdown, when the resonator is decoupled from its vibrational power. A sustained amplitude is observed for up to 8 seconds. Though the exact source of this anomaly remains elusive, it is suggested that it might include modal coupling and/or optomechanical effects.

Contents

Preface	i
Summary	ii
1 Introduction	1
1.1 Mechanical oscillator	2
1.2 Nonlinear dynamics	3
1.3 Observations from literature	3
1.3.1 Nonlinear damping	3
1.3.2 Mode coupling	4
1.4 Goals of the research	4
2 Paper	6
3 Conclusion and recommendations	14
3.1 Conclusion	14
3.2 Recommendations	14
3.2.1 Modelling	14
3.2.2 Experimental	14
Appendix A: Method	18
.1 SiN nanobeams	18
.2 Setup	18
.2.1 Process	18
Appendix B: Measurements	19

1

Introduction

Damping has engaged engineers over centuries. Dynamical motion tends to evolve towards a thermal equilibrium with their surroundings. A dynamical system is often considered to convert energy with the so-called environmental bath in the form of heat [1]. This applies for system on macro-scale, where a moving car will eventually come to a stop, as well as for micro-scale where vibrations are damped and energy dissipated.

Damping in general can also be a major restraint in performance and stability for e.g. sensing devices and signal processing. Furthermore, such systems must be susceptible to changes in the environment. Therefore shrinking resonators down to nanoscale therefore massively improves the responsivity. Therefore nano-electromechanical systems (NEMS) have found their application in innumerable sensitive detectors, such as force [2], mass [3], pressure [4] and spin detectors [5]. This process of miniaturization comes at the cost of the increased susceptibility of energy dissipation of the mechanical system and nonlinearities in the dynamical behavior.

In micro- and nanoelectromechanical systems, even relatively small vibration amplitudes exhibit nonlinearities. These can arise from the restoring force as well as the friction, which too can become amplitude dependent [6]. Such damping forces can comprise both intrinsic aspects such as Akhiezer [7], thermoelastic [8], and viscoelastic [9] damping, as well as extrinsic factors including support losses [10] and external interactions [11]. Since dissipation can have so many origins and can also behave nonlinearly, singling out one source from another will be especially challenging.

In addition, intermodal coupling can also greatly affect the rate of energy dissipation, which can even be enhanced near internal resonance (IR) [1]. This takes effect when the resonance frequency of two coupled eigenmodes have an integer ratio. In IR energy is transferred easily to different vibrational modes even when coupling is relatively small. Besides driving other modes this way and therefore affecting the resonators behavior, one mode can act as an energy sink for another mode, increasing the other modes effective dissipation rate.

The relevance of mode coupling extends to the ringdown phase, where a system undergoes free decay. Free response in itself offers a great means to extract crucial parameters such as mass, (non-linear) stiffness, and (nonlinear) damping rate in single mode systems [12]. However in combination with mode coupling, energy redistribution among modes can introduce intriguing deviations in decay behavior. Notably, cases have been identified where the route of dissipation exhibits an energy dependency, resulting in enhanced dissipation rates for high-energy states [13]. On the contrary, instances have been documented wherein energy is fed back into the observed mode, sustaining its amplitude for a brief period of time [14, 15].

This thesis provides a brief exploration of both linear and nonlinear dynamics in Sections 1.1 and 1.2, respectively. Following this, Section 1.3 delves into peculiarities from the existing literature. This chapter ends with the research question introducing the paper.

In chapter 2, the paper focuses on experimental evidence of anomalous energy decay in extremely low damped, highly nonlinear resonators during ringdown. The initial stage of the decay is marked by a sustained amplitude of the first harmonic, while thereafter the dissipation rate is increased and proceeds linearly. This lasts up to 8 seconds and is suggested to be caused by either or mode-coupling or optomechanical back-action. Chapter 3 provides recommendations and the conclusion of the research process.

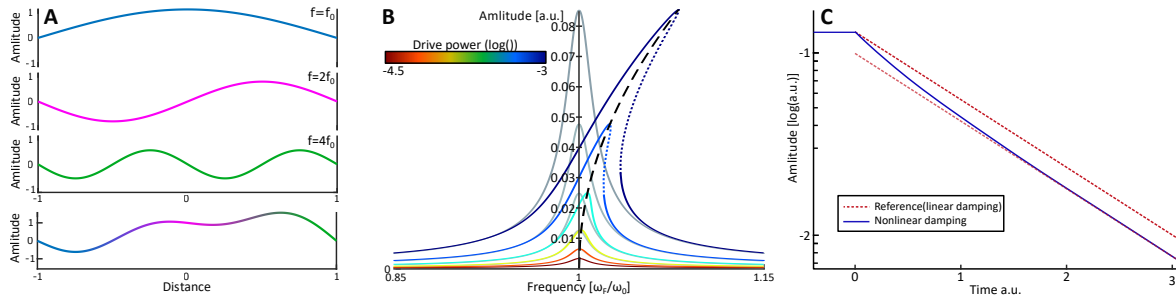


Figure 1.1: Vibration of mechanical resonator

A) The overall movement and shape of a resonator can often be deconstructed out of its modeshapes and corresponding frequencies. B) An example of a duffing resonator with mode hardening, with increased vibration amplitude the resonance is shifting as well. C) Ringdown of nonlinear resonators can exhibit nonlinear damping besides the linear component. At high amplitudes the vibration is more heavily damped, thereafter it revert to a linear behavior [12].

1.1. Mechanical oscillator

Before diving deep on the silicon nitride resonator, and particularly its nonlinear behavior and anomalous phenomenon, let us start first with a more general approach to vibrational systems.

The overall dynamics of a physical system, like a beam or string resonator, can often be described by a displacement function $w(x, y, z, t)$, but it can quickly become quite complex (figure 1.1A). Therefore is the motion often expanded by separation of variables [16], meaning that the function w is divided into N linear eigenmodes $\phi_i(x, y, z)$ and its time dependent generalized coordinates $q_i(t)$, such that $w(x, y, z, t) = \sum_i^N q_i(t)\phi_i(x, y, z)$, where i is the mode number. When the modeshape ϕ is normalized having a maximum of 1, then $q_i(t)$ describes vibration amplitude of that eigenmode. In linear dynamics these eigenmodes are so-called orthogonal, thus independent of each other with no energy transfer between them.

Let us scale down a little bit and look into a single mode. This also describes a basic resonator in its most elementary form, often approximated by a mass-spring system. Described by Newton's second law, the spring force, $-kx$, acting on mass, m , leads to the alteration of the velocity of the mass, \dot{x} . The equations of motion of such system would be:

$$m \frac{d^2 x(t)}{dt^2} + kx(t) = 0 \quad (\text{or} \quad m\ddot{q}_i(t) + kq_i(t) = 0) \quad (1.1)$$

This system has already been thoroughly investigated, and the solution involve the position of the mass oscillating at the fundamental frequency $\omega_0 = \sqrt{k/m}$. In a physical system energy is being dispersed so this equation is often complemented with a linear friction term $F_d = c\dot{x}$. In mechanics, frequently a dimensionless quality factor, $Q = \frac{m\omega_0}{c}$, is used to quantify the dissipative term. This dimensionless number effectively express the number of oscillations of a system before losing most of its vibrational energy in free oscillation. This means the higher the number, the lower the dissipation per cycle. In a resonator this loss of energy is usually restored by a (periodic) force, $F(t) = F \cos \omega_d t$, where F is the drive amplitude and ω_d is the corresponding frequency.

When all of these terms are included in equation 1.1, the equation of the linear harmonic oscillator emerges:

$$\ddot{x}(t) + \tau\dot{x} + \omega_0^2 x(t) = \bar{F} \cos \omega_d t \quad (1.2)$$

Here τ , ω^2 and \bar{F} are c , k and F divided by mass m respectively. Also this expanded system is well-understood, and the (driven) steady-state amplitude solution scales directly linearly with the applied force (increasing the force directly increases the resulting oscillation amplitude) and the phase shift with the oscillatory force is independent of the force magnitude nor the oscillation amplitude. Although this is an approximation, it is often valid in practice. Because substantial damping and mechanical failure before the threshold, the nonlinear response cannot be reached by most resonators.

On the other hand, scaling down allows us to produce structures that can easily reach oscillation amplitudes where the dynamic response cannot be described by such harmonic oscillator.

1.2. Nonlinear dynamics

On the larger scale, the linear approximation holds for it requires immense forces to overcome the high levels of damping and bring the system into nonlinear regime. As scaling down improves properties such as responsivity, it also allows the system to show nonlinearities. Relatively large amplitudes induce stresses for example that modulate the effective stiffness [17, 18]. This results in additional terms in the equation of motion such as a Duffing term, γq^3 , and nonlinear friction, like $\tau_{nl} q^2 \dot{q}$. The last is where the damping is enhanced while the amplitude increases [19]. These deviations from the linear model even allow for modal interactions, in which energy can be transferred from one mode of vibration to another.

The new model for the oscillator then would become:

$$\ddot{x}(t) + (\tau + \tau_{nl} x^2) \dot{x} + \omega_0^2 x(t) + \gamma x^3(t) = F \cos \omega_d t \quad (1.3)$$

The amplitude dependent stiffness has a noticeable effect on the systems dynamics, for with an increasing amplitude the effective stiffness becomes larger (for $\gamma > 0$) or lower (for $\gamma < 0$). This is either called spring hardening or spring softening respectively. When this model is plotted onto a figure, where the x-axis represent the drive frequency and the y-axis the steady state amplitude, figure 1.1B is generated. Here the drive frequency is normalized with respect to ω_0 , and the values of m , τ , τ_{nl} and γ are arbitrary (γ is chosen here to be positive). With an increased drive the effect of the Duffing term becomes apparent; The resonance frequency (the peak) shifts as the amplitude of the resonator increases too.

Ringdown, or free vibration, serves as a valuable tool for characterizing vibrational systems. It inherently comprises components at modal eigenfrequencies. Linear and nonlinear damping can easily be obtained (as can be seen in figure 1.1C) [12]. Considering nonlinear stiffness, the relationship between instantaneous frequency and amplitude, is also defining the underlying structure of the characteristic curve known as the backbone curve (dashed line in figure 1.1B). This curve reveals how the frequency will evolve during ringdown. Tracking the vibration amplitude the linear damping parameter is easily extracted [12]. It also allow to swiftly capture non-monotonic behavior induced by nonlinearities in the system [20]

As mentioned in section 1.1 a system's motion is not always captured by a single degree of freedom and due to nonlinearities energy can transfer between eigenmodes. This is called intermodal coupling, originating from the coupling potential U_{cp} . The motion of one mode is generating a periodic force on another mode [21]. This becomes especially important when the eigenfrequencies of the considered modes match up in an integer ratio, often a 1:3 or 1:2 ratio. In that case one mode can drive the other one into resonance, which is called internal resonance (IR).

In IR the second mode q_j must be considered in the equation of motion. So with the nonlinear terms included too this converges to the following equation [1]:

$$\begin{aligned} \ddot{q}_i + (\tau_i + \tau_{nl,i} q_i^2) \dot{q}_i + \omega_{0i}^2 q_i + \gamma q_i^3 + \frac{\partial U_{cp}}{\partial q_i} &= F_i(q_i, t) \\ \ddot{q}_j + \tau_j \dot{q}_j + \omega_{0j}^2 q_j + \frac{\partial U_{cp}}{\partial q_j} &= 0 \end{aligned} \quad (1.4)$$

Where i and j are distinctive coupled modes. A strong interaction in IR results in peculiar transient behavior in free response characterized by the energy exchange between modes. In the subsequent chapter this phenomenon undergoes further exploration and analysis from literature as well as a more elaborated examination on the origins of nonlinear damping.

1.3. Observations from literature

Prior to conducting measurements, a comprehensive literature survey is undertaken. This survey involves acquiring a principal understanding of various damping mechanisms, followed by an assessment of specific discoveries in ringdown research.

1.3.1. Nonlinear damping

Damping plays a pivotal role in determining the response of a device, and various mechanisms can contribute to the effective quality factor, Q^{-1} . In nanomechanics damping can have different origins and this section includes various means explained by an example from research papers.

Viscoelastic damping. This form of friction originates from the combination of elastic and viscous properties of the resonator material. Where the first is the restoration force after deformation while the

second is a form of drag to the velocity. For nonlinear models this form of friction is too considered inherently nonlinear [22]. This property is a major cause of damping for polymers [23].

Thermoelastic damping (TED), arises from the coupling of elastic modes with thermal phonons (vibrational waves in a crystal lattice). It becomes significant in every material where thermal variations are linked to (strain-induced) volume changes (thermal expansion), combined with a reasonable dispersion rate. This material property can be largely influenced by the modeshape [8], the resonator's dimensions, and the ambient temperature [6, 24].

Akhiezer damping is a phenomenon involving energy flow between phonon modes. In nanomechanical systems, vibrations are quantized into discrete phonon modes. A low-frequency eigenmode is coupled to high frequency phonons and when these modes interact, energy is dispersed from higher-frequency phonon modes to lower-frequency phonon modes [6]. This form of damping also scales with size and ambient temperature.

Clamping losses occur through the resonator's base or substrate, where acoustic phonons tunnel through the substrate, acting as a thermal bath. Research indicates that acoustic radiation loss is highly dependent on mode number [25]. Optimizing substrate design can mitigate this loss [26].

Surface losses are various losses attributed to the interaction of the resonator and the environment. Air, roughness or contact can induce a fair amount of friction [25]. **Two-level systems** are caused by defects in the material at a fairly low temperature [27]. **Electrostatic forces** impact nonlinear resonator behavior, which can tune multiple aspects of the resonator but can too introduce amplitude-dependent damping [28].

1.3.2. Mode coupling

Modal coupling is caused by the nonlinear coupling potential, U_{cp} . In combination with internal resonance (IR), condition where the ratio of resonance frequencies forms a rational number, a strong intricate nonlinear behavior is originated. IR can be created by careful design [29], by electrostatic tuning [13], by using the amplitude-frequency relation [1] or a combination to bring the resonator into a $n:m$ relationship ($n\omega_1 = m\omega_2$).

Tracking one mode in the vicinity of IR, the coupling increases and more energy is sapped to the second mode; the effective nonlinear damping will increase significantly [1].

In ringdown, a coupled mode can show different trajectories of how the energy is distributed over time. Observations from a 3:1 graphene resonator show that as the system reaches high energetic vibrations, modes couple and hybridize, leading to joint decay of modes $((\tau_1 + \tau_2)/2)$. The decay rate and coupling strength decrease over time, causing the modes to decouple (τ_1 and τ_2 separately) [13]. In general the linear damping of a higher frequency mode is larger than that of a lower one ($\tau_1 \ll \tau_2$). In a theoretical analysis [30] the energy of the first mode is dispersed through its linear damping and by the energy exchange with the highly damped coupled mode such that the overall damping increases.

To the contrary, a reversed phenomenon at IR is observed by [14] and [15], storing energy in the second mode such that the second mode acts as a "mechanical battery" and giving back energy to the first mode. Consequently a coherence time, $\tau_{coherent}$, is introduced, the duration where the amplitude of mode 1 is preserved. After that time the modes run out of phase and decouple. If one mode is transferring energy to the other mode faster than it is receiving, this mode will decrease faster than the linear thermalization. During the other mode will experience a slower decay than its linear rate. Together the energy in total is still being dispersed due to other mechanisms [20].

1.4. Goals of the research

This thesis is focused on the dynamics of nonlinear nanoresonators and specifically on the nonlinear damping characteristic in the vicinity of internal resonance. As seen in the research of Keşkekler [1] the nonlinear damping increases significantly near IR, which is largely in agreement with the research of Güttinger [13] and Shoshani [30].

Accordingly one would expect that nonlinear damping enhances near IR, yet the works of Chen [14] and Wang [15] report differently. Their research found sustained oscillation for a period of time after the periodic drive was shut off. And [15] goes even further recording coupling and sustained oscillation only moments after the ringdown initiated.

For this research the dynamics of a beam resonator will be investigated. Firstly by dynamic characterization, followed by amplitude measurements whilst the resonator experience free decay. These findings are presented in a scientific paper format in the following chapter. After which, in chapter 3,

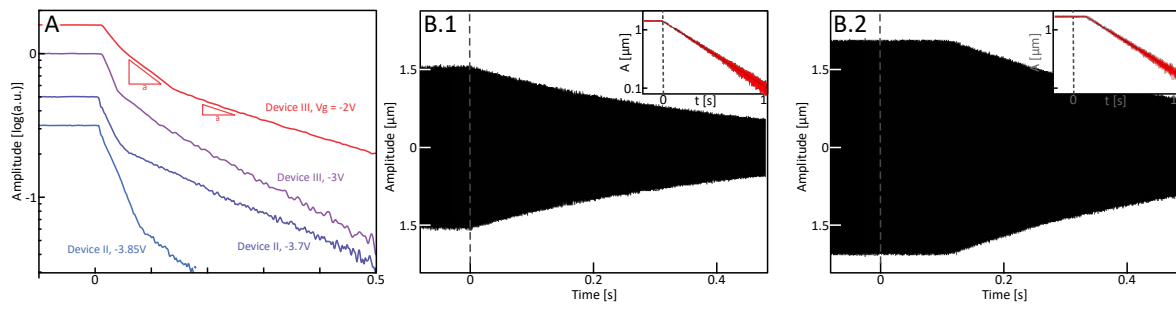


Figure 1.2: | Mode coupling in ringdown. A) Mode coupling causes a hybridization of mode 1 and 2, enhancing the damping of the measured mode. After the energy is depleted the modes decouple[13]. B) A clear preservation of vibration amplitude is observed at a higher starting amplitudes, where energy exchange between modes allow one mode to be sustained [14, 15].

the conclusion and recommendations concerning this research can be found. Additional information about the method and extra measurements can be found in the Appendices.

2

Paper

This chapter contains the main matter of the research, presented in a scientific paper format.

Ringdown of high-Q nonlinear Si_3N_4 beam resonator with multi-overtone recording*

Bart Schoone

Dynamics of Micro and Nano Systems, High-Tech Engineering

Delft University of Technology

(Dated: February 9, 2024)

Micro- and nanoelectromechanical (MEM/NEM) resonators are used in numerous fields of engineering and are crucial for time keeping, synchronization, and sensing applications. These systems are subjected to energy dissipation, which is a limiting factor in the performance. Extensive understanding is essential when nonlinearities show up in both stiffness and dissipation, to design appropriately. Focusing on dissipative mechanisms, this paper explores the vibrational behavior of a suspended clamped-clamped beam fabricated from silicon-nitride in the nonlinear regime. This study reveals a notorious decay in ringdown, when the resonator is decoupled from its vibrational power. A sustained amplitude is observed for up to 8 seconds. Though the exact source of this anomaly remains elusive, it is suggested that it might include modal coupling and/or optomechanical effects.

I. INTRODUCTION

Micro- and nanomechanical resonators are critical for time keeping components, synchronization [1], and sensing applications. For sensors, scaling down to the nanoscale enhances the responsivity, leading to their widespread application in sensitive detectors for force [2, 3], mass [4, 5], pressure [6], and spin detectors [7]. These sensors are constrained by the intensity of dissipation. In addition, the assumption of linearity breaks down due to the small size and enormous aspect ratios. Tiny oscillations can already introduce an amplitude dependent stiffness and exhibit nonlinear damping. Contemporary sensors still often avoid the nonlinear domain for their complex dynamics and dissipation mechanisms [2].

The study of energy dissipation has captivated researchers across various fields of physics. A physical system is often simply assumed to be coupled to the environmental bath, without fully understanding the origins and effects of this dispersion [8]. Knowing the sources of damping is fundamental for the utilization of the entire spectrum in the field of engineering and its applications. Damping can be intrinsic, like Akhiezer [9], thermoelastic [10] and viscoelastic damping [11], as well as extrinsic, support losses [12] and external interactions [13]. This attributes to the behavior of the resonator. Yet, untangling one source from the other can be a daunting task, for damping can stem from multiple origins simultaneously.

Besides dispersion to the environment through various mechanisms, energy can also be redistributed among eigenmodes of the system. This can be perceived as strong nonlinear damping for the measured mode, notably in the vicinity of internal resonance (IR) [14]. At IR, modes interact strongly and takes place only when the ratio of the frequencies of the coupled modes is an

integer. The significance of mode coupling is also visible in the free response, where the system is decoupled from the drive. Different linear and nonlinear parameters can be extracted by using the free vibration response, i.e. the stiffness, Duffing parameter and the damping parameters, both linear and nonlinear [15]. When modal coupling is present in the system, specifically in or near IR, energy is easily being redistributed among modes, generating an anomalous decay as the vibrational amplitude evolves [16]. On the one hand, research found that the path of dissipation is energy dependent, such that for high energy states the dissipation rate is enhanced [17]. On the other hand, studies found energy being delivered back to the observed mode, such that the amplitude remains steady for a short period of time [8, 18].

In this work, we also experimentally show an anomalous decay of a micromechanical resonator. The highly nonlinear resonator shows a sustained amplitude during the initial stages of the ringdown. Using the lock-in technique we measure the contribution of different overtones during ringdown and find that the first harmonic experiences a greatly reduced damping for up to 8 seconds. After this the decay rate increases as expected and proceeds linearly. The cause of this phenomenon is tried to track down but remains elusive. The origins of the anomaly are suggested to lie within either mode-coupling or optomechanical back-action.

II. RESULTS

The experimental setup involves a suspended clamped-clamped beam resonator. It is fabricated from silicon nitride (Si_3N_4), measuring $4\mu\text{m}$ by 96nm , with a length of $1300\mu\text{m}$. The resonator is set approximately $6\mu\text{m}$ above the silicon (Si) substrate, which is forming the backplane. The structure is placed onto a piezo stack and enclosed within a vacuum chamber, where the pressure is reduced to $2e - 6\text{mBar}$.

The equipment used for measurement, includes a commercially available Polytec MSA400 Laser Doppler

* This paper is a part of the Masters thesis of the author

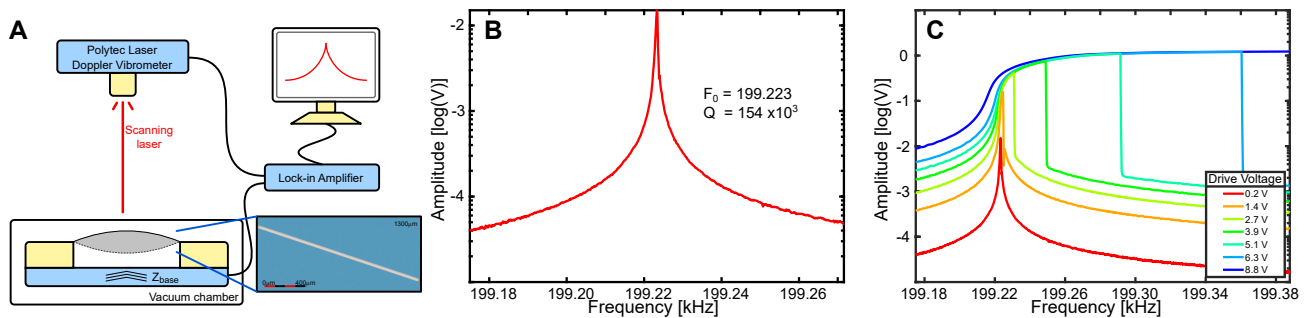


FIG. 1 | **Schematic set-up, linear frequency sweep and nonlinear frequency sweep.** A, Measurement set-up schematic: The SiN string resonator inside a vacuum ($1e-5$ mBar) chamber excited with a piezo base actuator. Measured from top view by a red laser by the Polytec MSA400 and processed by the ZI HF2LI. B, Linear direct frequency response curve (motion amplitude versus drive frequency) of the first harmonic. C, Direct frequency response curves of the first harmonic with increased driving amplitude, resulting in nonlinear behavior

Vibrometer (LDV), fitted with a red sensing laser with a wavelength of $\lambda = 633\text{nm}$. A Zurich Instruments HF2LI Lock-In Amplifier is utilized for data acquisition and processing and to actuate the piezostack. A schematic of the setup is depicted in Figure 1a. More details in Appendix A.

To characterize the beam resonator the piezo is driven by the alternating voltage generated by the Lock-In Amplifier. By sweeping the frequency of the voltage from a low to a higher frequency, the frequency response curve is characterized. This curve presents the resulting amplitude response at various frequency steps, enabling the determination of several key parameters, like eigenfrequency and linear damping rate. For high enough amplitudes and multiple measurements this also allow the determination of the Duffing and the nonlinear damping rate [14]. The natural frequency of the clamped-clamped beam is measured to be around 199.223 kHz. Due to the non-constant ambient temperature the resonance varies slightly. The parameter of the linear damping rate ($2\Gamma\dot{x}$) is determined to be $\Gamma_{ss}/2\pi \approx 0.648$ Hz. Consequently, the quality factor (Q) is found to be approximately 154×10^3 , as illustrated in Figure 1b.

Upon increasing the drive power, the motion of the microbeam rises to the point where linear approximations are no longer valid. For clamped-clamped beams, nonlinearities can already arise from its geometry, where a mass is attached to two linear springs [19]. The amplified drive voltage can lead to amplitude-dependent stiffness, nonlinear damping behavior, and modal coupling. By incrementally elevating the drive amplitude, we obtained the nonlinear frequency response, which is presented in Figure 1c. For increased response amplitude the resonance frequency is progressed with the drive frequency, establishing a high-energy state, before falling down to the low-amplitude branch. At first glance, this curve closely resembles the behavior of a typical Duffing resonator.

The curve presented in Figure 1c serves as the basis for our energy decay measurements. By driving the resonator using the piezo stack, we actuate the resonator

in an out-of-equilibrium state. Subsequently, by switching off the driving force while the system is in a steady state, we monitor the decay of vibrational energy using the LDV.

Ringdown is a valuable probe for evaluating nonlinear dissipation. To observe the free decay of the resonator in the nonlinear regime, we can employ two methods. The first method would be to determine the highest steady state amplitude per drive voltage and measure the decay turning of the drive at that point. When in the nonlinear (Duffing) regime, this means to approach the saddle-node bifurcation, just before the high-amplitude state ceases to exist. In figure 1c this measurement point would then be just before the amplitude drops down. A second method would be to drive the resonator with a fixed high drive voltage and measure the ringdown at various points on the Duffing curve. Both methods allow different starting amplitudes to be measured, however, the latter method offers greater resilience to minor variations in temperature or pressure, which may cause shifts in resonance and the saddle node's position.

Figure 2A displays the full frequency sweep at 8.8 V. Herein the specific frequencies and corresponding amplitudes are highlighted at which the driving force is switched off. Subfigure 2B depicts the normalized amplitude, where all measurements are scaled with respect to the highest steady state power, pointing out the observed trend.

Starting in the lower amplitude regime (denoted as point A to the left of the figure), the system exhibits almost linear behavior during the free response, as shown in Figure 2B, line A. Here, we monitor the amplitude of the fundamental harmonic. The resonator is driven up to $t = t_{off}$, after which the piezo is shut off and the resonator undergo a free decay. The linear damping coefficient can easily be determined using the exponential decay formula $a = a_0 e^{-\Gamma t}$ [15]. This value can be cross-verified with the results obtained from the frequency response curve, yielding a linear damping rate of $\Gamma_{rd}/2\pi = 0.840$ Hz.

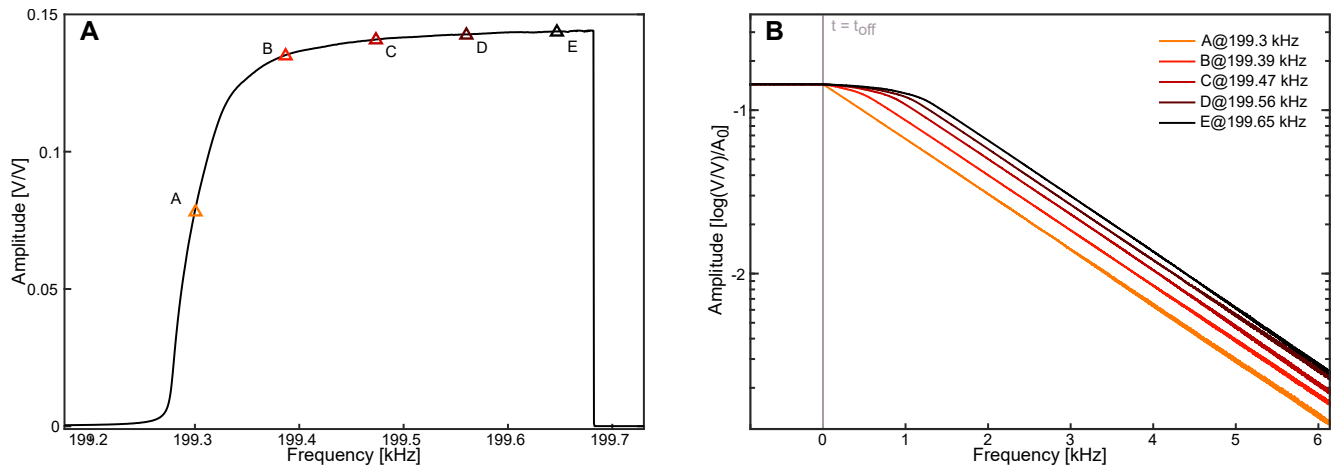


FIG. 2 | **Ring-down measurement of the SiN string resonator.** A. Direct frequency response curve of the nonlinear first harmonic driven at 8.8V. The letters A-E are different spots at which an energy decay measurement is executed. Where A is still in linear regime despite the high driving power, further into the curve the nonlinearity increases. B. The decay process for different swept frequencies and thus amplitudes. All starting amplitudes are set equal to the highest value (point E). The difference in decay rate is extended the further the frequency is swept

As we progress along the nonlinear frequency response curve, we conduct ringdown measurements at points B to E. The steady state amplitude of lines A to E are normalized such that their amplitude while driven are set equal. This way the deviations are more noticeable; Line B in Figure 2B is already displaying slight nonlinearity in ringdown, showing a different path than its lower amplitude predecessor. This effect is more pronounced at higher amplitudes. The observed decay rate in the first stage is strongly reduced for a considerable time, before the amplitude shows a similar line like line A, the linear decay. This effect is observed for an elongated period up to 7s in current configuration. Higher powers also resulted in an even longer two-staged ringdown. Notably, the resonance frequency shifts during the ringdown process, necessitating the use of a wide signal filtering bandwidth. This approach prevents data loss in the extensive frequency range where vibrational energy is dissipated, however, this also increases the noise level. We have also observed this phenomenon in similar resonators with the same cross-section and anchor point but varying lengths (more detail in Section III).

III. DISCUSSION

Our observations show a distinct two-stage dissipation with the initial stage exhibiting a strongly reduced decay rate. The examined literature do not show direct similarities to these observations (figure 3A). The phenomenon can be attributed to several factors including mode coupling and optomechanical effects. Where mode coupling is specific to the resonator, optomechanical effects are caused by the interaction of setup (e.g. measurement laser) and resonator. In the following paragraphs

both are elaborated more. The two-staged slope even show similarities to two-level system defects described by [20] (Appendix B). However, these types of sustained oscillation can only occur at extremely low temperatures ($< 4K$) [21, 22].

Our research shows similarities with (non-)linear mode coupling as described in the research by C. Chen et al. [18], M. Wang et al. [8] and in a mirrored manner with the work of Güttinger et al. [17]. These authors describe their observations as a consequence of mode coupling. For a system to observe strong modal coupling, at least two of the vibrational eigenmodes need to get close to internal resonance (IR). This means that one eigenmodes frequency is an integer multiple of the other eigenmodes frequency ($n\omega_i = m\omega_j$). When a perfect string is considered, the eigenmodes are aligned at an integer value. Assuming a perfect string, similar with a guitar string for example, has its eigenmodes aligned an integer value apart from the primary resonance.

Both Chen [18] and Wang [8] define a system where the higher harmonic can be used as a sort of a mechanical battery, a storage such that the modal energy can be redistributed towards the observed harmonic. As a result, the observed mode maintains its amplitude after the system is decoupled from the drive. For a moment of time, coupled modes provide enough energy to sustain and even increase the vibrational amplitude of this harmonic. After the so-called coherence time, the harmonics decouple and decay separately. The composition of the eigenmodes make the coupling such that the first mode decay is negated in its entirety in high amplitude region. On the other hand, the work of Güttinger et al. [17] describes a coupling revealing the opposite. They describe a hybridized decay rate, where the energy of the first harmonic is distributed. This mode experiences an enhance

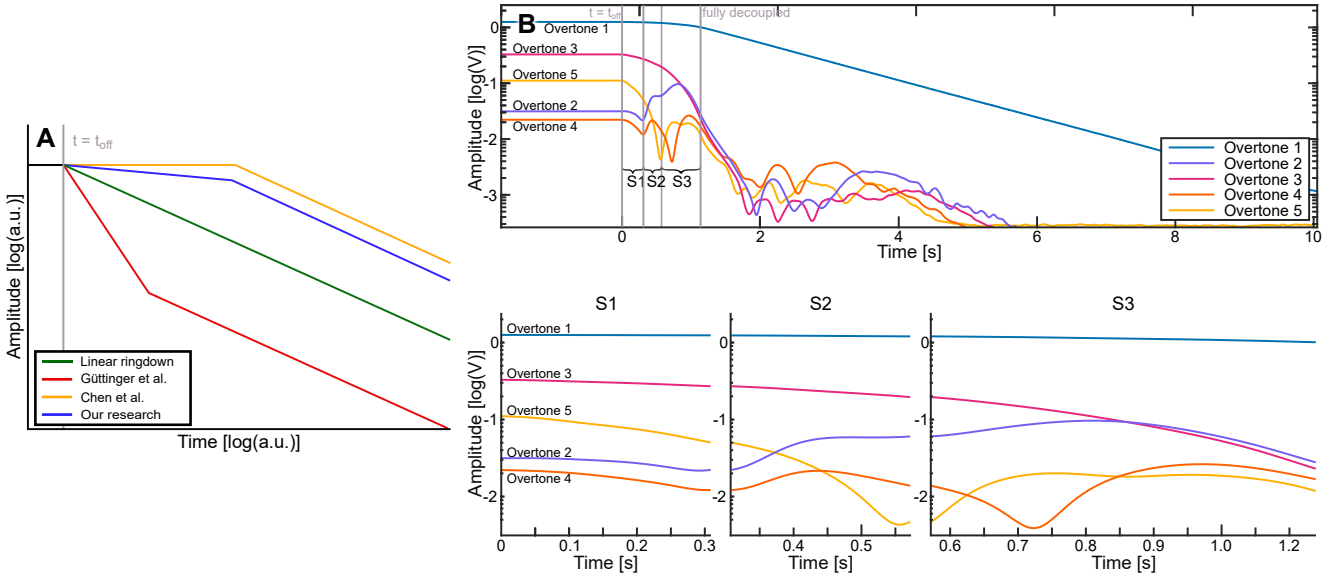


FIG. 3 | **Experimental decay rates and measured overtones.** A. Schematic visualisation of findings in literature [8, 17, 18] (logarithmic scale), B. Measured free response with overtones, data is averaged with a moving Gaussian. The decay at the top can be separated in 4 sections after decoupling with the drive. The first three sections the overtones show an intricate decay while the primary overtone is sustained, while the last section display a linear decay of the primary overtone.

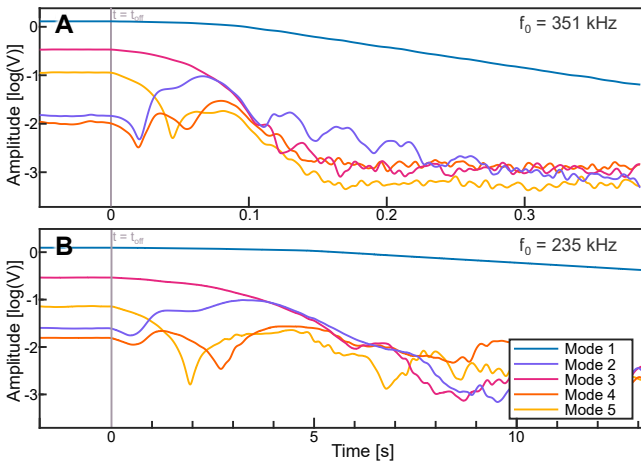


FIG. 4 | **Two other strings.** A. String of length 700 μm with f_0 around 351kHz, B. String of length 1100 μm and f_0 around 235 kHz. Both showing similar behavior of higher modes in a different time frame

damping in high energy state. A global representation of the work of Chen et al. and Güttinger et al. is offered in figure 3A. In this work the decay rate is only reduced in comparison to a fully sustained one.

To gain deeper insights into the mechanism governing the exchange of energy within our system, our measurement setup has been configured to capture higher-order data as well. The input of the Lock-In Amplifier can be multiplied by different references simultaneously.

This allows for measuring multiple harmonics at the same time (Figure 3B). In the research conducted by Chen et al., they harnessed the concept of resonant mode coupling to facilitate the transfer and storage of mechanical energy across various vibrational modes. Subsequently, this energy is redistributed back to the principal mode during free response. Notably, this phenomenon translates to a faster depletion of energy in higher modes, influenced by both the (non-)linear decay rate and the dynamic exchange of energy between the third mode and the primary mode.

Figure 3B shows the first 5 overtones observed at $n\omega_0$, where ω_0 is the primary modes eigenfrequency. The 4 higher overtones are also nonzero while powered. At $t = t_{off}$ (after 1.7s in figure 3B) the external excitation is terminated. The overall amplitude of the first overtone is sustained for up to 1.2s before the decay progresses linearly. For ease the ringdown is separated into 3 sections (S1-3). In the first section all the modes are losing amplitude at each a different rate. In comparison, with the third section the third mode also seems to sustain the amplitude, while still an observable decay is visible. After about 0.6 seconds the decay of the third overtone seem to increase. The same appears for overtone 5 in section 1 and 2, however overtone 5 gains amplitude in section 3 and decays freely thereafter. Even more remarkable are the lines describing overtones 2 and 4. Both gain amplitude in section 2 and cross overtone 5 in amplitude. In the last section before "decoupling", the amplitude of overtone 2 increases even more to match overtone 3. The amplitude of 5 surpasses overtone 4 again here at the

lower end. Only the first 6 overtones are recorded (overtone 6 not showing any significance), overtone 7, being an odd overtone, might show again similarly with overtone (1), 3 and 5.

A similar intricate decay has also been observed in other strings. The length of sustained amplitude seems to be a function of amplitude, frequency and Q-factor (more details in Appendix B). Figure 4 show other strings of 700 μm and 1100 μm respectively. These strings have different resonance and different Q-factors but the manner of decay seems similar. The time the decay rate is diminished, however, is various.

When modal coupling is considered as primary means of sustaining the primary mode, one can argue that energy is being transferred between modes. The decrease in amplitude of overtone 3 and overtone 5 seem to match in that sense that energy is pumped into the primary mode. This is in accordance with the simulations of the Fermi-Pasta-Ulam-Tsingou problem, where first mode's vibrations of a string first distribute vibrational energy among higher modes and after a while the energy is transferred back to the first mode. In an ideal situation only the odd modes are actuated this way and all the energy is transferred back to mode 1. In non-ideal systems even harmonics can be actuated as well and energy is also transferred to the environmental bath [19, 23].

On the other hand, figure 3B shows also similarities with mechanical overtones and frequency combs described by De Jong et al. [24]. In their research, the back-action is described between the mechanics and the optical properties of the cavity. This is caused by the partial optical transparency of the used material and the (partial) reflectivity of the backplane. The incoming laser is reflected and forming a standing wave with the incoming light. The resonator used in our experiments, silicon nitride, and the backplane, silicon, have a reflectivity of about 30% and 35% respectively for the used wavelength of $\lambda = 633\text{nm}$ [24]. The laser is parallel to the motion of the resonator, which is therefore moving through the induced nonlinear optical field. This can induce different optomechanical back-action being photothermal [25], radiation pressure [21] and dielectrophoretic [24] forces.

When a (powerful) light source or laser is focused on a material, some of its energy will be absorbed by the material in the form of heat. The photothermal effect is laser-induced heating, which in turn changes the tension in the material due to the thermal expansion. Si_3N_4 is very susceptible to (local) change in temperature. In a string resonator this is causing the frequency to shift substantially for example. For a resonator which is subjected to a periodic optical intensity [14] or which is moving through an optical field [25], the fluctuations in tension can induce a parametric driving force. Although the probe laser is not powerful ($p \leq 3\text{mW}$ [24]) a slight frequency change is observed over time after the laser is turned on, assuming a temperature change due to the incident laser. This may explain the reduced rate

of dissipation of the first observed mode, the system is parametrically pumped by the probing laser. However the boost is not sufficient to fully sustain the vibration. The amplitude still decays at a low rate to the point where the pumping is no longer possible.

The optomechanical interference can also lead to a radiation pressure force. Basically using photons to transfer momentum into the resonator. For this effect to take place in a substantial matter, a cavity must be created where light can be trapped such that the total adds up [21]. Therefore this phenomenon is very unlikely to be apparent in our set-up: the backplane is not highly reflective and the string is not acting like an optical trap.

Another back-action force can also be exerted on the Si_3N_4 resonator if the initial motion is in the order of $> \lambda/4$. The combination of the dielectric property of Si_3N_4 and the electromechanical optical field generated by the standing wave is generating a dielectrophoretic force on the resonator. This force is proportional to the gradient of the optical intensity. Accordingly the additional force switches direction twice per optical peak the resonator passes at high amplitude. This $2n$ (number of peaks) periodic force is generating motion components at $n\omega_0$. This force is not directly imposing additional energy to the system or institute negative nonlinear damping but it would explain the higher order overtones of the system seen in figure 3B.

IV. CONCLUSION

This paper has delved into the dynamics of the suspended clamped-clamped beam fabricated from silicon nitride, with a focus on vibrational dissipative behavior. The initial characterization the beam provided parameters such as natural frequency, linear damping rate and quality factor. Driving it with higher excitation showed considerable nonlinearities notably an amplitude-dependent stiffness in the frequency sweep. Subsequent investigation consisted of analysis of the free response of the resonator, unveiling intriguing phenomena, particularly a reduced decay rate. This observation was attributed to potential factors, as mode coupling and optomechanical effects, accentuating the complexity.

Firstly, parallels were drawn with prior research on mode coupling, which found an enhanced or a fully cancelled out damping rate of the first mode for a short period of time. As shown, the reduced damping rate in our system can last up to seconds. However, the complexity of the observed dynamics, among which amplitude, frequency and Q-factor dependence, presented challenges for achieving a comprehensive understanding.

Additionally, optical effects were considered. These included photothermal effect, radiation pressure and dielectrophoretic forces. While the first concept can be accounted for the reduced dissipation rate, the latter could be the source of the higher harmonics visible.

The experimental findings do raise broader questions about the interplay of various factors in vibrational dynamics. Further research may include an extensive analysis on mode coupling (e.g. STEP method [26]) or analysis on optomechanical interference with simulations. Also another measurement technique (other laser frequency

or intensity, could help unveiling the true source of the anomaly found in this paper.

also may exclude can help uncovering the anomalous phenomena and advancing the field of microscale mechanical systems.

-
- [1] D. Antonio, D. H. Zanette, and D. López, “Frequency stabilization in nonlinear micromechanical oscillators,” *Nature Communications*, vol. 3, 2012. [Online]. Available: www.nature.com/naturecommunications
- [2] A. Bachtold, J. Moser, and M. I. Dykman, “Mesoscopic physics of nanomechanical systems,” 2022. [Online]. Available: <http://arxiv.org/abs/2202.01819>
- [3] J. Moser, J. Güttinger, A. Eichler, M. J. Esplandiú, D. E. Liu, M. I. Dykman, and A. Bachtold, “Ultrasensitive force detection with a nanotube mechanical resonator,” *Nature Nanotechnology*, vol. 8, pp. 493–496, 2013. [Online]. Available: www.nature.com/naturenanotechnology
- [4] J. Chaste, A. Eichler, J. Moser, G. Ceballos, R. Rurali, and A. Bachtold, “A nanomechanical mass sensor with yoctogram resolution,” *Nature Nanotechnology*, vol. 7, pp. 301–304, 2012. [Online]. Available: www.nature.com/naturenanotechnology
- [5] K. L. Ekinci, Y. T. Yang, and M. L. Roukes, “Ultimate limits to inertial mass sensing based upon nanoelectromechanical systems,” *Journal of Applied Physics*, vol. 95, pp. 2682–2689, 2004. [Online]. Available: <https://doi.org/10.1063/1.1642738>
- [6] M. Šiškins, M. Lee, D. Wehenkel, R. van Rijn, T. W. de Jong, J. R. Renshof, B. C. Hopman, W. S. J. M. Peters, D. Davidovikj, H. S. J. van der Zant, and P. G. Steeneken, “Sensitive capacitive pressure sensors based on graphene membrane arrays,” *Microsystems Nanoengineering*, vol. 6, p. 102, 12 2020. [Online]. Available: www.nature.com/micronanohttp://www.nature.com/articles/s41378-020-00212-3
- [7] J. Moser, A. Eichler, J. Güttinger, M. I. Dykman, and A. Bachtold, “Nanotube mechanical resonators with quality factors of up to 5 million,” *Nature Nanotechnology*, vol. 9, pp. 1007–1011, 2014. [Online]. Available: www.nature.com/naturenanotechnology
- [8] M. Wang, D. J. Perez-Morelo, D. Lopez, and V. A. Aksyuk, “Persistent nonlinear phase-locking and non-monotonic energy dissipation in micromechanical resonators,” 2022.
- [9] K. Kunal and N. R. Aluru, “Akhiezer damping in nanostructures,” *Physical Review B - Condensed Matter and Materials Physics*, vol. 84, 2011.
- [10] R. Lifshitz and M. Roukes, “Thermoelastic damping in micro- and nanomechanical systems,” *Physical Review B - Condensed Matter and Materials Physics*, vol. 61, pp. 5600–5609, 2000.
- [11] S. Zaitsev, O. Shtempluck, E. Buks, and O. Gottlieb, “Nonlinear damping in a micromechanical oscillator,” *Nonlinear Dynamics*, vol. 67, pp. 859–883, 2012.
- [12] G. D. Cole, I. Wilson-Rae, K. Werbach, M. R. Vanner, and M. Aspelmeyer, “Phonon-tunnelling dissipation in mechanical resonators,” *Nature Communications*, vol. 2, 2011. [Online]. Available: www.nature.com/naturecommunications
- [13] R. B. Bhiladvala and Z. J. Wang, “Effect of fluids on the q factor and resonance frequency of oscillating micrometer and nanometer scale beams,” *Physical Review E - Statistical, Nonlinear, and Soft Matter Physics*, vol. 69, 2004.
- [14] A. Keşkekler, O. Shoshani, M. Lee, H. S. van der Zant, P. G. Steeneken, and F. Alijani, “Tuning nonlinear damping in graphene nanoresonators by parametric–direct internal resonance,” *Nature Communications*, vol. 12, 2021. [Online]. Available: <https://doi.org/10.1038/s41467-021-21334-w>
- [15] P. Polunin, Y. Yang, J. Atalaya, E. Ng, S. Strachan, O. Shoshani, M. Dykman, S. Shaw, and T. Kenny, “Characterizing mems nonlinearities directly: The ring-down measurements,” *2015 Transducers - 2015 18th International Conference on Solid-State Sensors, Actuators and Microsystems, TRANSDUCERS 2015*, pp. 2176–2179, 2015.
- [16] O. Shoshani, S. W. Shaw, and M. I. Dykman, “Anomalous decay of nanomechanical modes going through nonlinear resonance,” *Scientific Reports*, vol. 7, 2017. [Online]. Available: www.nature.com/scientificreports/
- [17] J. Güttinger, A. Noury, P. Weber, A. M. Eriksson, C. Lagoin, J. Moser, C. Eichler, A. Wallraff, A. Isacsson, and A. Bachtold, “Energy-dependent path of dissipation in nanomechanical resonators,” *Nature Nanotechnology*, vol. 12, pp. 631–636, 2017. [Online]. Available: www.nature.com/naturenanotechnology
- [18] C. Chen, D. H. Zanette, D. A. Czaplewski, S. Shaw, and D. López, “Direct observation of coherent energy transfer in nonlinear micromechanical oscillators,” *Nature Communications*, vol. 8, 2017. [Online]. Available: www.nature.com/naturecommunications
- [19] A. Keşkekler, “Nonlinear coupling and dissipation in two-dimensional resonators,” Ph.D. dissertation, Delft University of Technology, 2023.
- [20] X. Dong, M. I. Dykman, and H. B. Chan, “Strong negative nonlinear friction from induced two-phonon processes in vibrational systems,” *Nature Communications*, vol. 9, 2018. [Online]. Available: www.nature.com/naturecommunications
- [21] V. Singh, O. Shevchuk, Y. M. Blanter, and G. A. Steele, “Negative nonlinear damping of a multilayer graphene mechanical resonator,” *PHYSICAL REVIEW B*, vol. 93, p. 245407, 2016.
- [22] F. Hoehne, Y. A. Pashkin, O. Astafiev, L. Faoro, L. B. Ioffe, Y. Nakamura, and J. S. Tsai, “Damping in high-frequency metallic nanomechanical resonators,” 2010.
- [23] T. Jansen, “Mode coupling in nanomechanical string resonators,” 2021.
- [24] M. H. J. D. Jong, A. Ganesan, A. Cupertino, and R. A. Norte, “Mechanical overtone frequency combs,” 2022.

- [25] R. A. Barton, I. R. Storch, V. P. Adiga, R. Sakakibara, B. R. Cipriany, B. Ilic, Si, P. Wang, P. Ong, P. L. Mceuen, J. M. Parpia, and H. G. Craighead, "Photothermal self-oscillation and laser cooling of graphene optomechanical systems," 2012. [Online]. Available: <https://pubs.acs.org/sharingguidelines>
- [26] A. Keşkekler, V. Bos, A. M. Aragón, P. G. Steeneken, and F. Alijani, "Multimode nonlinear dynamics of graphene resonators," *Phys. Rev. Appl.*, vol. 20, p. 064020, Dec 2023. [Online]. Available: <https://link.aps.org/doi/10.1103/PhysRevApplied.20.064020>

Conclusion and recommendations

3.1. Conclusion

This thesis has delved into the investigation of the suspended clamped-clamped beam fabricated from silicon-nitride, revealing nonlinearities and intriguing phenomena. As explained in the introduction, this included amplitude dependent stiffness, nonlinear damping and possible mode coupling.

With a focus on the vibrational dissipative behaviour, the system showed unusual decay in ring-down. A reduced decay rate was observed when the drive was turned off when a certain steady state amplitude was reached. In ringdown, the first harmonic was sustained for a relatively long period of time. Including higher harmonics suggested a complex interplay eigenmodes through mode coupling or, as later argued, effects induced by the measurement laser.

Subsequently, the paper remains inconclusive and further investigation is needed to pinpoint the sources of the anomaly. Should modal coupling be identified as the root cause, this research would be a start for designing mechanical batteries, storing energy in higher modes. Conversely, if the anomaly originates from the optical domain, the laser induced harmonics may be used as tool in metrology and timing applications.

3.2. Recommendations

Based on the findings and discussions presented in this work, the following recommendations are proposed:

3.2.1. Modelling

- Generating a comprehensive understanding concerning modal coupling would include using the STEP method proposed by [31]. This method involves Finite Element modelling (e.g. using Comsol) to work towards a linear reduced order model. Using that to extract interactions and form a nonlinear model which includes multi modal interaction. Analysing and simulations would then shed light on modal energy transfer during ringdown.
- Laser-induced self-actuation may be simulated by using the model provided by [32]. The temporal distribution of the optical field has its interactions with the motion of the beam resonator. Their model includes this periodic dielectrophoretic force on silicon nitride. Simulation in time of the undriven system would then possibly show overtones and the anomaly as observed during measurements.

3.2.2. Experimental

Additional measurements could also shed light on the observations:

- Conduct frequency sweep and ringdown measurements under varied conditions, different than drive power, frequency and pressure. Specifically, adjusting probe laser power or frequency to impact the material differently, following insights from [32].
- The interaction among higher harmonics, as discussed in Chapter 2, suggests that driving higher harmonics into resonance could result in strong coupling. The hypothesized energy exchange from higher harmonics back to the first mode during ringdown might also induce reciprocal interactions when only a higher mode is actuated. Furthermore a driven higher mode would involve even higher order interactions.

- Address any potential significance of the "Auxiliary" warning light on data integrity. This might be caused by sensor saturation, though the software of the PSV would have captured this. Some measurements found coherence in the observations and the auxiliary light.

By combining experimental investigations with detailed modelling, a comprehensive understanding of the underlying mechanisms can be gained. These steps can serve as a framework to determine whether the observed response stems from modal coupling, optical effects, or it may even reveal novel influences that may not have been previously considered.

Bibliography

- [1] Ata Keşkekler et al. “Tuning nonlinear damping in graphene nanoresonators by parametric–direct internal resonance”. In: *Nature Communications* 12 (1 2021). ISSN: 20411723. DOI: 10.1038/s41467-021-21334-w. URL: <https://doi.org/10.1038/s41467-021-21334-w>.
- [2] J Moser et al. “Ultrasensitive force detection with a nanotube mechanical resonator”. In: *Nature Nanotechnology* 8 (7 2013), pp. 493–496. ISSN: 17483395. DOI: 10.1038/nnano.2013.97. URL: www.nature.com/naturenanotechnology.
- [3] J Chaste et al. “A nanomechanical mass sensor with yoctogram resolution”. In: *Nature Nanotechnology* 7 (5 2012), pp. 301–304. ISSN: 17483395. DOI: 10.1038/nnano.2012.42. URL: www.nature.com/naturenanotechnology.
- [4] Makars Šiškins et al. “Sensitive capacitive pressure sensors based on graphene membrane arrays”. In: *Microsystems Nanoengineering* 6 (1 Dec. 2020), p. 102. ISSN: 2055-7434. DOI: 10.1038/s41378-020-00212-3. URL: www.nature.com/micronano%20http://www.nature.com/articles/s41378-020-00212-3.
- [5] J Moser et al. “Nanotube mechanical resonators with quality factors of up to 5 million”. In: *Nature Nanotechnology* 9 (12 2014), pp. 1007–1011. ISSN: 17483395. DOI: 10.1038/nnano.2014.234. URL: www.nature.com/naturenanotechnology.
- [6] Adrian Bachtold, Joel Moser, and M I Dykman. “Mesoscopic physics of nanomechanical systems”. In: (2022). URL: <http://arxiv.org/abs/2202.01819>.
- [7] K Kunal and N R Aluru. “Akhiezer damping in nanostructures”. In: *Physical Review B - Condensed Matter and Materials Physics* 84 (24 2011). ISSN: 10980121. DOI: 10.1103/PhysRevB.84.245450.
- [8] Ron Lifshitz and M. Roukes. “Thermoelastic damping in micro- and nanomechanical systems”. In: *Physical Review B - Condensed Matter and Materials Physics* 61 (8 2000), pp. 5600–5609. ISSN: 1550235X. DOI: 10.1103/PhysRevB.61.5600.
- [9] Stav Zaitsev et al. “Nonlinear damping in a micromechanical oscillator”. In: *Nonlinear Dynamics* 67 (1 2012), pp. 859–883. ISSN: 0924090X. DOI: 10.1007/s11071-011-0031-5.
- [10] Garrett D Cole et al. “Phonon-tunnelling dissipation in mechanical resonators”. In: *Nature Communications* 2 (1 2011). ISSN: 20411723. DOI: 10.1038/ncomms1212. URL: www.nature.com/naturecommunications.
- [11] Rustom B Bhiladvala and Z Jane Wang. “Effect of fluids on the Q factor and resonance frequency of oscillating micrometer and nanometer scale beams”. In: *Physical Review E - Statistical, Non-linear, and Soft Matter Physics* 69 (3 2 2004). ISSN: 1063651X. DOI: 10.1103/PhysRevE.69.036307.
- [12] P. Polunin et al. “Characterizing MEMS nonlinearities directly: The ring-down measurements”. In: *2015 Transducers - 2015 18th International Conference on Solid-State Sensors, Actuators and Microsystems, TRANSDUCERS 2015* (November 2016 2015), pp. 2176–2179. DOI: 10.1109/TRANSDUCERS.2015.7181391.
- [13] Johannes Güttinger et al. “Energy-dependent path of dissipation in nanomechanical resonators”. In: *Nature Nanotechnology* 12 (7 2017), pp. 631–636. ISSN: 17483395. DOI: 10.1038/nnano.2017.86. URL: www.nature.com/naturenanotechnology.
- [14] Changyao Chen et al. “Direct observation of coherent energy transfer in nonlinear micromechanical oscillators”. In: *Nature Communications* 8 (2017). ISSN: 20411723. DOI: 10.1038/ncomms15523. URL: www.nature.com/naturecommunications.
- [15] Mingkang Wang et al. “Persistent nonlinear phase-locking and non-monotonic energy dissipation in micromechanical resonators”. In: ()).

- [16] Ron Lifshitz and M C Cross. *Nonlinear Dynamics of Nanomechanical and Micromechanical Resonators*. 2009, pp. 1–52. ISBN: 9783527407293. DOI: 10.1002/9783527626359.ch1.
- [17] D. Davidovikj et al. “Nonlinear dynamic characterization of two-dimensional materials”. In: *Nature Communications* 8 (1 2017). ISSN: 20411723. DOI: 10.1038/s41467-017-01351-4.
- [18] Hidde Jelger Robbert Westra. *Nonlinear Beam Mechanics*. 2012, p. 16. ISBN: 9789085931331. URL: <https://repository.tudelft.nl/islandora/object/uuid%3A6a67595f-5983-4325-8df9-b1f628d4877f>.
- [19] A Eichler et al. “Nonlinear damping in mechanical resonators made from carbon nanotubes and graphene”. In: *Nature Nanotechnology* 6 (6 2011), pp. 339–342. ISSN: 17483395. DOI: 10.1038/nnano.2011.71. URL: www.nature.com/naturenanotechnology.
- [20] Oriël Shoshani and Steven W Shaw. “Resonant modal interactions in micro/nano-mechanical structures”. In: *Nonlinear Dynamics* 104 (3 2021), pp. 1801–1828. ISSN: 1573269X. DOI: 10.1007/s11071-021-06405-3. URL: <https://doi.org/10.1007/s11071-021-06405-3>.
- [21] Keivan Asadi, Jun Yu, and Hanna Cho. “Nonlinear couplings and energy transfers in micro-and nano-mechanical resonators: Intermodal coupling, internal resonance and synchronization”. In: *Philosophical Transactions of the Royal Society A: Mathematical, Physical and Engineering Sciences* 376 (2127 2018). ISSN: 1364503X. DOI: 10.1098/rsta.2017.0141.
- [22] Marco Amabili. “Derivation of nonlinear damping from viscoelasticity in case of nonlinear vibrations”. In: *Nonlinear Dynamics* 97 (3 2019), pp. 1785–1797. ISSN: 1573269X. DOI: 10.1007/s11071-018-4312-0. URL: <https://doi.org/10.1007/s11071-018-4312-0>.
- [23] S Schmid and C Hierold. “Damping mechanisms of single-clamped and prestressed double-clamped resonant polymer microbeams”. In: *Journal of Applied Physics* 104 (9 2008), p. 93516. ISSN: 00218979. DOI: 10.1063/1.3008032. URL: <https://doi.org/10.1063/1.3008032>.
- [24] B H Houston, D M Photiadis, and M H Marcus. “Thermoelastic loss in microscale oscillators ARTICLES YOU MAY BE INTERESTED IN”. In: *Cite as: Appl. Phys. Lett* 80 (2002), p. 1300. DOI: 10.1063/1.1449534. URL: <https://doi.org/10.1063/1.1449534>.
- [25] L G Villanueva and S Schmid. “Evidence of surface loss as ubiquitous limiting damping mechanism in SiN micro- and nanomechanical resonators”. In: *Physical Review Letters* 113 (22 2014). ISSN: 10797114. DOI: 10.1103/PhysRevLett.113.227201.
- [26] Y Taturyan et al. “Ultracoherent nanomechanical resonators via soft clamping and dissipation dilution”. In: *Nature Nanotechnology* 12 (8 2017), pp. 776–783. ISSN: 17483395. DOI: 10.1038/nnano.2017.101. URL: www.nature.com/naturenanotechnology.
- [27] C Seoáñez, F Guinea, and A H Castro Neto. “Dissipation in graphene and nanotube resonators”. In: *Physical Review B - Condensed Matter and Materials Physics* 76 (12 2007). ISSN: 10980121. DOI: 10.1103/PhysRevB.76.125427.
- [28] Alexander Croy et al. “Nonlinear damping in graphene resonators”. In: *Physical Review B - Condensed Matter and Materials Physics* 86 (23 2012). Crossover from linear to nonlinear damping. Phononic dissipation, p. 235435. ISSN: 10980121. DOI: 10.1103/PhysRevB.86.235435.
- [29] Atabak Sarrafan, Behraad Bahreyni, and Farid Golnaraghi. “Development and Characterization of an H-Shaped Microresonator Exhibiting 2:1 Internal Resonance”. In: *Journal of Microelectromechanical Systems* 26 (5 2017), pp. 993–1001. ISSN: 10577157. DOI: 10.1109/JMEMS.2017.2710322. URL: http://www.ieee.org/publications_standards/publications/rights/index.html.
- [30] O Shoshani, S W Shaw, and M I Dykman. “Anomalous decay of nanomechanical modes going through nonlinear resonance”. In: *Scientific Reports* 7 (1 2017). ISSN: 20452322. DOI: 10.1038/s41598-017-17184-6. URL: www.nature.com/scientificreports/.
- [31] Ata Keşkekler et al. “Multimode Nonlinear Dynamics of Graphene Resonators”. In: *Phys. Rev. Appl.* 20 (6 Dec. 2023), p. 064020. DOI: 10.1103/PhysRevApplied.20.064020. URL: <https://link.aps.org/doi/10.1103/PhysRevApplied.20.064020>.
- [32] Matthijs H J De Jong et al. “Mechanical overtone frequency combs”. In: (2022).

Appendix A: Method

In this chapter additional information is provided concerning procedures during the experiments.

.1. SiN nanobeams

The silicon chip is provided with a set of silicon-nitride nanobeams with varying lengths. Which have the a width of $6\mu\text{m}$, and a thickness of 92nm . The space inbetween beams is $800\mu\text{m}$. The different lengths are $100\mu\text{m}$, $300\mu\text{m}$, $700\mu\text{m}$, $1100\mu\text{m}$, $1300\mu\text{m}$, $1900\mu\text{m}$, $3100\mu\text{m}$. The beams are edged without anchor pads and with a cavity of around $2\mu\text{m}$ in depth. The beam resonators were previously used for other research in nonlinear dynamics. The beams are designed to have low damping and to show significant nonlinearities.

.2. Setup

Figure 1a of the paper shows the global setup of the system. The chip is put inside a vacuum chamber onto a piezoactuator mostly without double sided tape (a few measurements double sided tape was used). The piezoelement is connected to the outside to a Zurich Instruments HF2LI, 50MHz Lock-In Amplifier. A red laser (633nm) is used to detect the velocity of the resonator using laser Doppler vibrometry with a commercial Polytec Scanning Vibrometer (PSV). The output of the PSV is then fed to the HF2LI. The eigenfrequencies of the beams are easily found utilizing the PSV, but for further analysis the HF2LI is used. The velocity accuracy of the PSV is set to VD-09 500 mm/s/V.

.2.1. Process

First harmonics are recognised using the software provided with the PSV. This would serve a starting point when continuing the measurements with the Lock-in amplifier. High Q results in narrow resonance peaks, which are difficult to recognise when just sweeping the drive. Using the Lock-in acquisition technique higher harmonics can then be measured too. When the SiN beams are not yet acclimated, the frequency tends to shift due to temperature changes. Even the laser induced heat causes a significant frequency shift of the resonance of the beam.

Frequency sweeps are done to measure its resonance frequency again precisely and to observe the Duffing effect when driven to larger amplitudes. Seen in figure 1b and 1c of the paper, the nonlinear effect increases in frequency reach. At the same time different overtones can be tracked using the lock-in technique, by multiplying the incoming signal with a corresponding reference. The signal is mixed with a reference signal, which can also be a higher harmonic, and with the reference signal 90 degree out of phase. This gives the X and Y value respectively, the magnitude and phase difference of both give the vibration amplitude and phase of the signal. The reference frequency is also used as a drive output voltage.

When sweeping a small bandwidth is applied, so the frequency range over which the amplitude is averaged is smaller, but the settling time is larger. In ringdown the bandwidth must be larger, since the frequency is about to shift due the Duffing parameter, the bandwidth should be chosen accordingly.

Notably, at high vibration amplitudes the "auxiliary" light of the PSV was turned on. Though this output was not considered in measurements and was discarded being important.

Appendix B: Measurements

Different strings were measured in the process. Strings measuring $300\mu\text{m}$, $700\mu\text{m}$, $900\mu\text{m}$, $1100\mu\text{m}$, $1300\mu\text{m}$ and $1800\mu\text{m}$. The string of length $1300\mu\text{m}$ is already extensively discussed in the paper. Numerous measurements were conducted varying string length and drive power. Following are just a handful of measurements: Figure 1 shows ringdown measurements in a string of length $700\mu\text{m}$ when the initial drive is at 6V. At different point in the sweep curve, a ringdown is initiated, capturing overtones simultaneously.

Figure 2 shows multiple drive voltages and the ringdown of the first harmonic of the string of $1100\mu\text{m}$. Figure 3 shows yet other string resonators, though the exact data was not captured properly, they still show the phenomenon at 860kHz ($300\mu\text{m}$) and 136 kHz ($1800\mu\text{m}$).

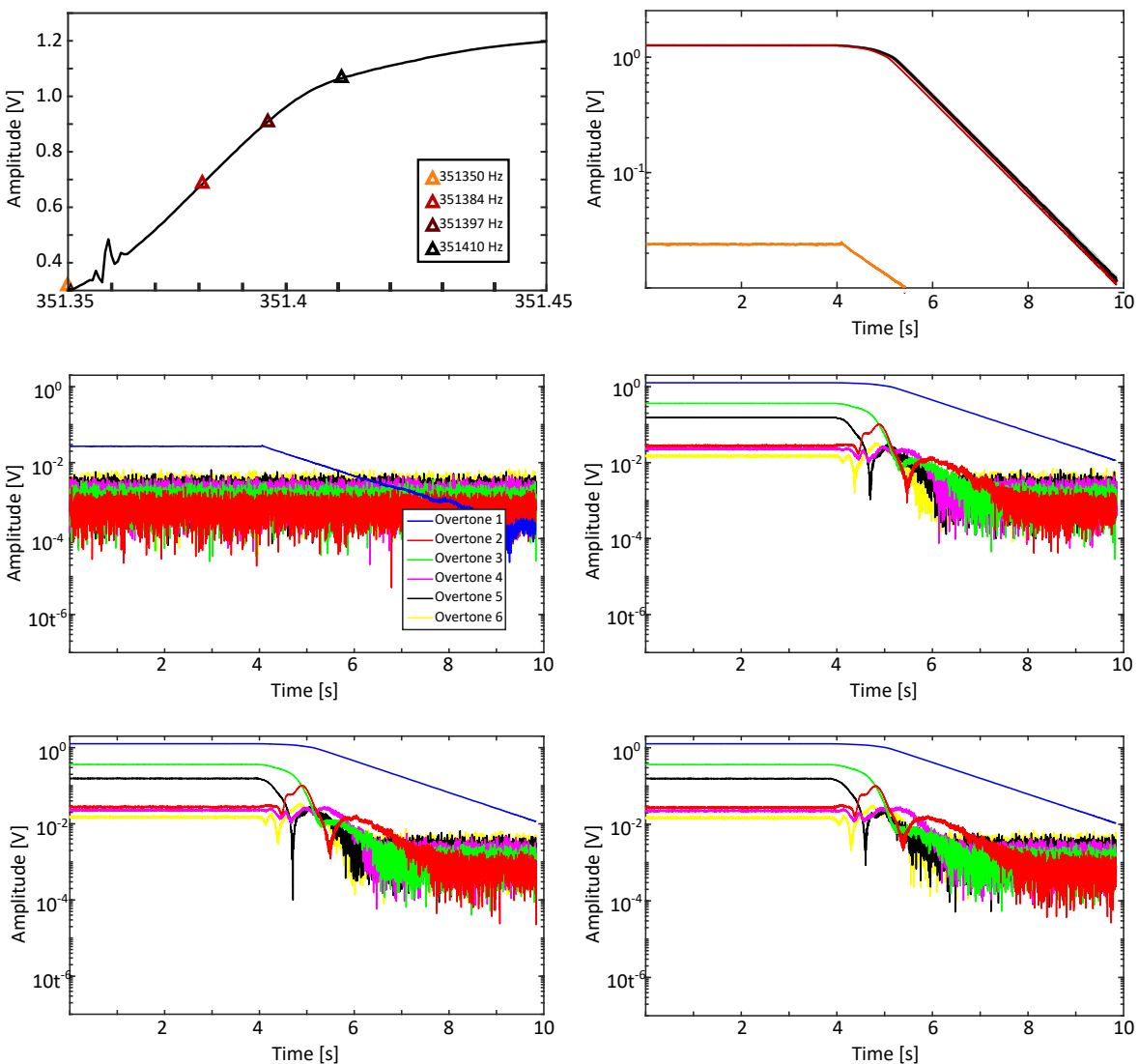


Figure 1: | $700\mu\text{m}$. Ringdown measurements of a string of length $700\mu\text{m}$ with an initial drive of 6V. Along the curve multiple steps are measured

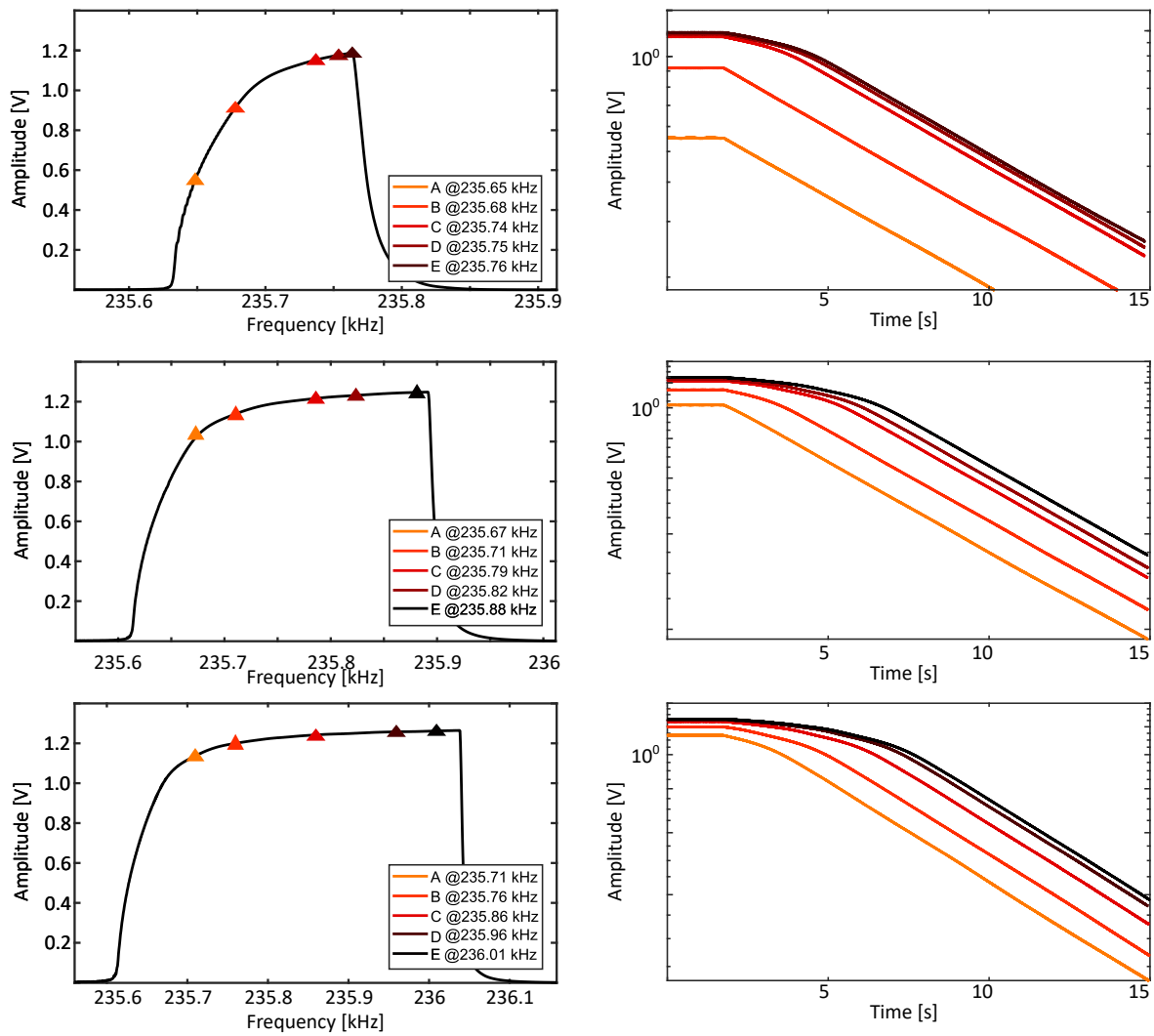


Figure 2: | $1100\mu\text{m}$. Ringdown measurements of a string of length $1100\mu\text{m}$ the drive voltage is varied while still measuring the ringdown at different frequencies

When the voltage was set to the maximum for the string of length $1100\mu\text{m}$, also the frequency sweep shows great anomalies. The dimple in the sweep is also recognisable in ringdown. The amplitude seem to follow the same route back while the frequency is slowly reduced due the decaying amplitude (figure 4).

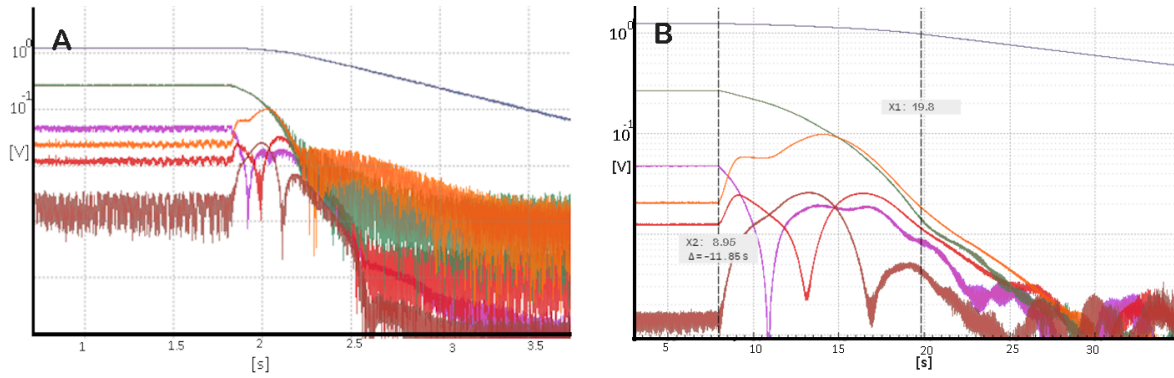


Figure 3: | $300\mu\text{m}$ and $1800\mu\text{m}$. Only a screenshot was properly saved. Both strings are driven at 10V at 860 kHz and 136 kHz respectively

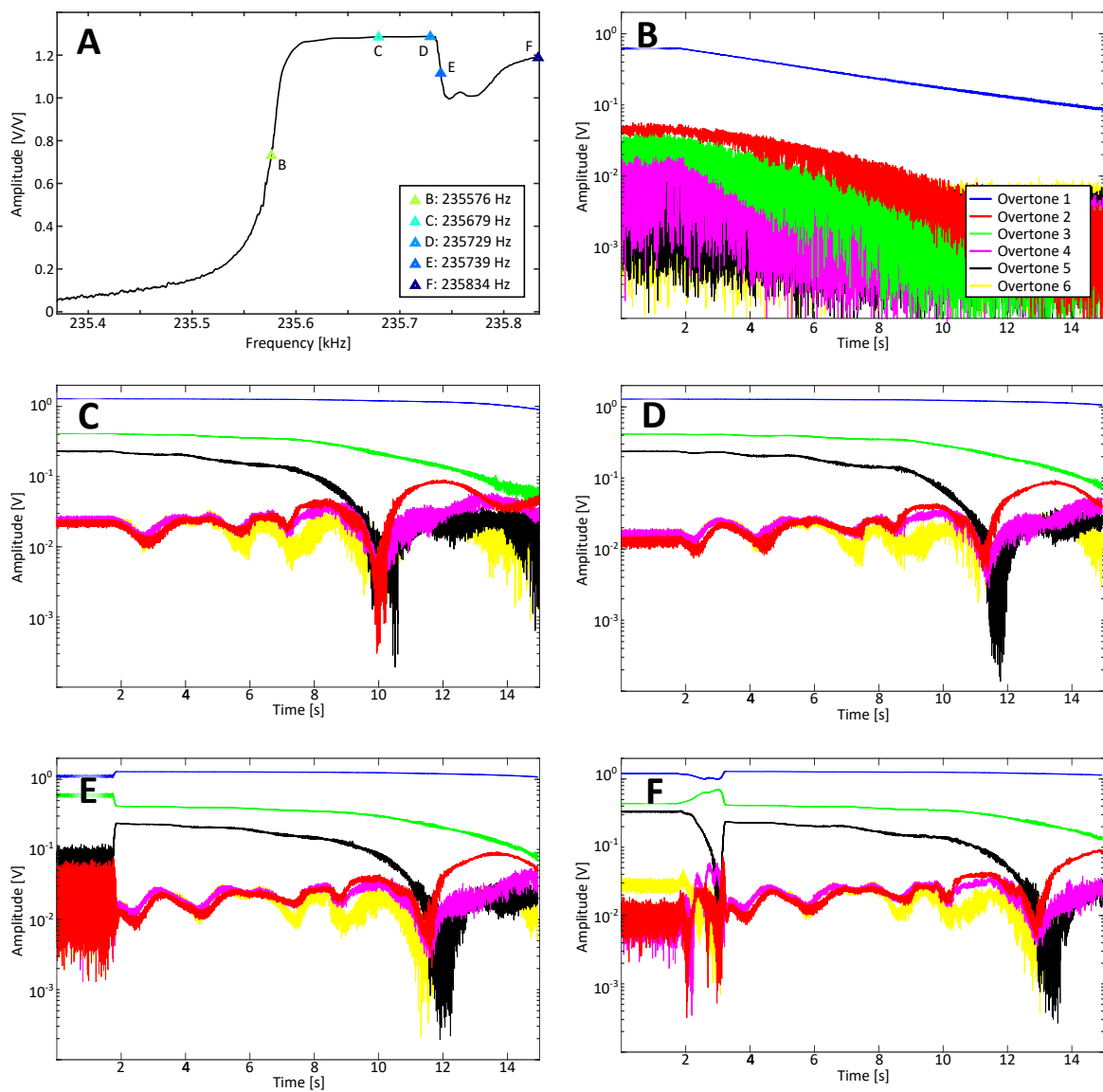


Figure 4: | $1100\mu\text{m}$. The voltage is set to maximum while the pressure